

Available online at www.sciencedirect.com

Advances in Space Research xxx (2006) xxx–xxx

**ADVANCES IN
SPACE
RESEARCH**
(a COSPAR publication)www.elsevier.com/locate/asr

First results of ozone profiles between 35 and 65 km retrieved from SCIAMACHY limb spectra and observations of ozone depletion during the solar proton events in October/November 2003

G.J. Rohen ^{a,*}, C. von Savigny ^a, E.J. Llewellyn ^b, J.W. Kaiser ^c, K.-U. Eichmann ^a,
A. Bracher ^a, H. Bovensmann ^a, J.P. Burrows ^a

^a *Institute of Environmental Physics (IUP), University of Bremen, Otto-Hahn-Allee 1, 28359 Bremen, Germany*

^b *Institute of Space and Atmospheric Studies, University of Saskatchewan, 116 Science Place, Saskatoon, Canada S7N 5E2*

^c *Remote Sensing Laboratories (RSL), University of Zurich, Winterthurer Str. 190, 8057 Zurich, Switzerland*

Received 19 October 2004; received in revised form 11 March 2005; accepted 12 March 2005

Abstract

Ozone density profiles between 35 and 65 km altitude are derived from scattered sunlight limb radiance spectra measured by the SCIAMACHY instrument on the Envisat satellite. The method is based on the inversion of normalized limb radiance profiles in the Hartley absorption bands of ozone at selected wavelengths between 250 and 310 nm. It employs a non-linear Newtonian iteration version of Optimal Estimation (OE) coupled with the radiative transfer model SCIARAYS. The limb scatter technique combined with a classical OE retrieval in the short-wave UV-B and long-wave UV-C delivers reliable results as shown by a first comparison with MIPAS V4.61 profiles yielding agreement within 10% between 38 and 55 km. An overview of the methodology and an initial error analysis are presented. Furthermore the effect of the solar proton storm between 28 October and 6 November 2003 on the ozone concentration profiles is shown. They indicate large depletion of ozone of about 60% at 50 km in the Northern hemisphere, a weaker depletion in the Southern hemisphere and a dependence of the depletion on the Earth's magnetic field.

© 2006 Published by Elsevier Ltd on behalf of COSPAR.

Keywords: SCIAMACHY; Ozone; Mesosphere; Retrieval technique; Solar proton event October 2003

1. Introduction

Emission and absorption spectroscopy are two techniques used to retrieve ozone profiles in the mesosphere: a common technique uses the airglow emissions of oxygen (Noxon, 1975; Llewellyn and Witt, 1977; Marsh et al., 2002, 2003). Another technique is the absorption spectroscopy by stellar occultation, e.g., Global Ozone Monitoring by Occultation of Stars (GOMOS) (Kyrölä, 2004), solar occultation, e.g., Halogen Occultation Experiment (HALOE) (Russell et al., 1993) or by scanning the limb

of the Earth, e.g., Optical Spectrometer and InfraRed Imaging System (OSIRIS) (Llewellyn et al., 2004). Rusch et al. (1984) have been the first to retrieve ozone profiles from limb observations. They used UV limb radiance profile measurements at 265.0 and 296.4 nm performed with an ultraviolet spectrometer on the Solar Mesosphere Explorer (SME) to infer ozone concentrations between about 48 and 65 km.

The significant absorption of solar radiation in the Hartley bands of ozone alters the UV limb radiance profiles within the 35–65 km tangent height range. Measurements of limb scattered radiance profiles can therefore be used to retrieve ozone concentrations in the upper stratosphere and lower mesosphere, if the selection of the wavelengths is done carefully.

* Corresponding author. Tel.: +49 421 218 4352; fax: +49 421 218 4555.
E-mail address: rohen@iup.physik.uni-bremen.de (G.J. Rohen).

51 2. SCIAMACHY on Envisat

52 The European Space Agency's (ESA) spacecraft Envi-
 53 ronmental satellite (Envisat) was launched on 1 March
 54 2002 from Kourou (French Guiana) into a sun-synchro-
 55 nous polar orbit with an inclination angle of 98.55° and
 56 a descending equator crossing local time of 10:00 am.
 57 SCanning Imaging Absorption SpectroMeter for Atmo-
 58 spheric Cartography (SCIAMACHY) (Bovensmann
 59 et al., 1999), one of the ten instruments on Envisat, is
 60 a spectrometer designed to measure transmitted, reflected
 61 and scattered sunlight in the wavelength region from 214
 62 to 2380 nm at a moderate spectral resolution of 0.24–
 63 1.48 nm. The instrument consists of eight grating spec-
 64 trometers and photo-diode array detectors. It measures
 65 the daylight radiance in limb and nadir viewing geome-
 66 try, and also solar or lunar light transmitted through
 67 the atmosphere in occultation mode. In limb mode the
 68 instantaneous field of view of SCIAMACHY is 0.045°
 69 in elevation (about 2.6 km at the tangent point) and
 70 1.8° in azimuthal direction (about 110 km). A typical
 71 limb scan cycle comprises 31 horizontal scans from the
 72 Earth's surface to 92 km with a duration of 1.5 s each.
 73 During a typical limb cycle duration the spacecraft
 74 moves about 400 km in the along-track direction. The
 75 instrument reaches global coverage within 6 days.

76 3. Retrieval method

77 The method used to recover ozone density profiles from
 78 SCIAMACHY observations follows that employed by
 79 Flittner et al. (2000) and McPeters et al. (2000) to retrieve
 80 ozone density profiles from the LORE/SOLSE limb scatter
 81 measurements in the Huggins absorption bands of ozone.
 82 A similar method, using the Chappuis bands of ozone,
 83 has been applied to retrieve stratospheric ozone profiles,

e.g., from OSIRIS (von Savigny et al., 2003) and SCIAM- 84
 ACHY limb scattering observations, using three combined 85
 wavelengths (Eichmann et al., 2004; von Savigny et al., 86
 2004b). 87

Fig. 1 shows the weighting functions for four selected 88
 wavelengths. They show the sensitivity of the wavelength 89
 dependent radiance profiles at each tangent height with 90
 respect to ozone concentrations. The figures show that 91
 there is no sensitivity below 35 km at wavelengths shorter 92
 than 310 nm. Currently the retrieval version V2.16 is run 93
 with 250, 252, 254, 264, 267.5, 273.5, 283, 286.5, 288, 94
 290, 305, 307 and 310 nm simultaneously by averaging 95
 the radiances over 2 nm wavelength intervals. The wings 96
 of Fraunhofer lines and dayglow emissions are considered. 97
 Emission line wavelengths are avoided. Expected emissions 98
 are the NO- γ bands ($A^2\Sigma^+ \rightarrow X^2\Pi$), which are the most 99
 prominent emission features in the UV, the N₂ Vegard- 100
 Kaplan bands ($A^3\Sigma_u^+ \rightarrow X^1\Pi_g^+$), the N₂ second positive 101
 bands ($C^3\Pi_u \rightarrow B^3\Sigma_g^-$), atomic oxygen lines ($^2P \rightarrow ^4S$) at 102
 247.000 and 247.109 nm and ($^1S \rightarrow ^3P$) at 297.2 nm 103
 (López-Puertas, 2000). Other expected emissions from iron, 104
 sodium and magnesium can hardly be seen. Only the NO- γ 105
 bands play an important role. 106

The first step of the retrieval scheme consists of normal- 107
 ization of the limb radiance profiles 108

$$I_{i,k}^n = \frac{I_{i,k}}{I_{i,\text{ref}}}, \quad (1) \quad 110$$

with $I_{i,k}$ denoting the limb radiance at wavelength λ_i , 111
 $i \in \{1, \dots, 13\}$ and tangent height Th_k , $k \in \{1, \dots, 21\}$. 112
 $I_{i,\text{ref}}$ denotes the radiance at wavelength λ_i at the chosen 113
 reference tangent height. Each reference height is chosen 114
 at altitudes between 56 and 70 km. The effect of normal- 115
 ization is (a) to reduce the sensitivity to all disturbances 116
 which affect all wavelengths, e.g., clouds, and (b) not to 117
 use the absolute calibration of the instrument raw data. 118

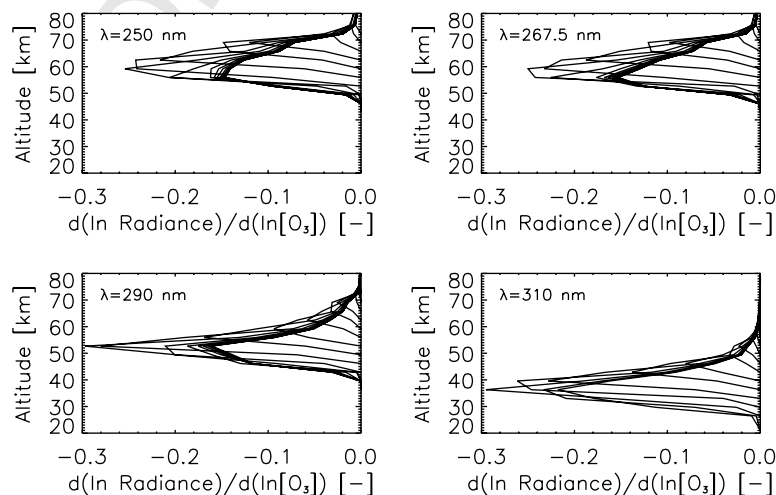


Fig. 1. Weighting functions of a sample ozone profile retrieval for four selected wavelengths, which show the sensitivity of the retrieval method from 35 to 65 km. Each curve represents the fractional sensitivity for a different tangent height from 20 to 80 km. The measurement was made on 12 March 2003. The solar zenith angle is 78.9°.

119 Therefore the normalization at wavelength-dependent
 120 tangent heights minimizes the possible impact of several
 121 error sources. The normalized radiance profiles are com-
 122 bined to a column vector $\mathbf{y} = (I_{i,k}^n)^T$. A non-linear New-
 123 ton iteration scheme of OE is used with the program
 124 package SCIARAYS, which has been developed especial-
 125 ly for the retrieval of trace gas concentrations from UV
 126 and visible (UV–vis) limb measurements (Kaiser, 2001).
 127 It contains a radiative transfer model and an instrument
 128 model and solves the integral form of the radiative trans-
 129 fer equation using fully spherical ray tracing, optional
 130 refractive bending and double-scattering. Weighting func-
 131 tions are derived analytically. Fig. 2 shows a fit of the
 132 modelled radiances for four selected wavelengths and
 133 the residuals for all wavelengths for a sample profile
 134 retrieval. Ozone absorbs very strongly in the Hartley
 135 bands, and model simulations showed, that surface
 136 reflection is negligible and multiple-scattering below
 137 310 nm contributes less than 5% and below 305 nm less
 138 than 1% to the radiances. Thus the reflected, the first
 139 reflected and then scattered radiation, and the second
 140 scattered radiation can be neglected.

141 The used temperature and pressure climatology is a
 142 compilation of several experimental datasets and model
 143 data (McPeters, 1993). The a priori ozone profiles for
 144 the inversion scheme are taken from the United King-
 145 dom Universities Global Atmospheric Modelling Pro-
 146 gramme (UGAMP) climatology based on five years of
 147 averaged SME, Stratospheric Aerosol and Gas Experiment
 148 II (SAGE II), and Solar Backscatter Ultra-Violet
 149 (SBUV) satellite data (Li and Shine, 1995). An a priori
 150 error of 80% was assumed and the a priori covariance
 151 matrix was assumed to be diagonal. The measurement
 152 error was estimated at 6%. Averaging kernels, which
 153 show, how the retrieved profiles dependent on the true

154 profile, and the vertical resolution of a sample profile
 155 retrieval can be seen in Fig. 3.

4. Error statistics 156

157 An overview of the relevant sources of error is given in
 158 Table 1. The largest error source is the residual pointing error
 159 of the Envisat orbit model propagator (von Savigny et al.,
 160 2005). To correct the tangent heights and therefore minimize
 161 the errors, a pointing retrieval using the *knee-technique* (Janz
 162 et al., 1996) was performed (Kaiser et al., 2004). This reduces
 163 the pointing precision from previously up to 3.5–0.3 km after
 164 the pointing-retrieval (von Savigny et al., 2005). With an
 165 assumed accuracy of the tangent heights of 0.5 km the esti-
 166 mated errors in the ozone profiles due to the tangent height
 167 inaccuracy are between 4 and 19%.

168 Additionally, mesospheric clouds, which occur at about
 169 83 km at high latitudes in the summer hemisphere (von
 170 Savigny et al., 2004a) are detected with an algorithm and
 171 the affected measurements are rejected.

4.1. Comparison with MIPAS results 172

173 Michelson Interferometer for Passive Atmospheric
 174 Sounding (MIPAS) (Fischer and Oelhaf, 1996) is a Fourier
 175 Transform Spectrometer (FTS) operating in limb-geometry
 176 in the infrared region from 4.15 to 14.6 μm with a high
 177 spectral resolution. The MIPAS operational products are
 178 provided by ESA and validated with ozone profiles, e.g.,
 179 from HALOE (V19) and SAGE II (V6.2) (Bracher et al.,
 180 2004), where the ozone profiles differ by about 5–15% from
 181 HALOE and SAGE II profiles. The validation in the work
 182 of (Bracher et al., 2004) is restricted to altitudes from about
 183 12–60 km, thus a validation with MIPAS only can give rea-
 184 sonable validation results with SCIAMACHY (V2.16)

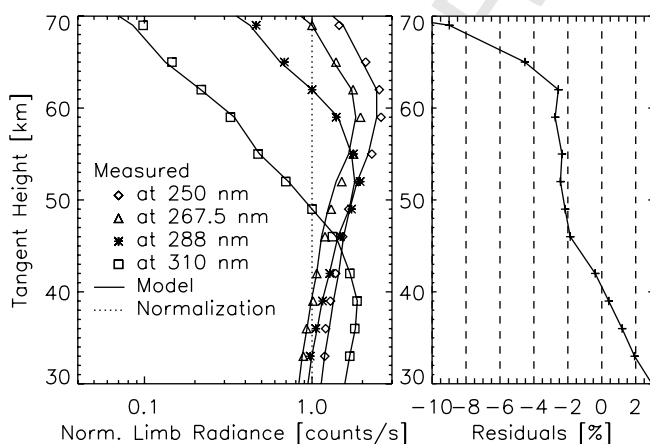


Fig. 2. (Left panel) Newton iteration fit of measured to modelled radiances at four wavelengths for the same sample profile retrieval as in Fig. 1. The dotted line indicates the normalization points. The normalization point of the measurement at 250 nm is located at 76 km and cannot be seen in this figure. (Right panel) Corresponding residual for all wavelengths is below 3%, except above 62 km, where they exceed more than 5%.

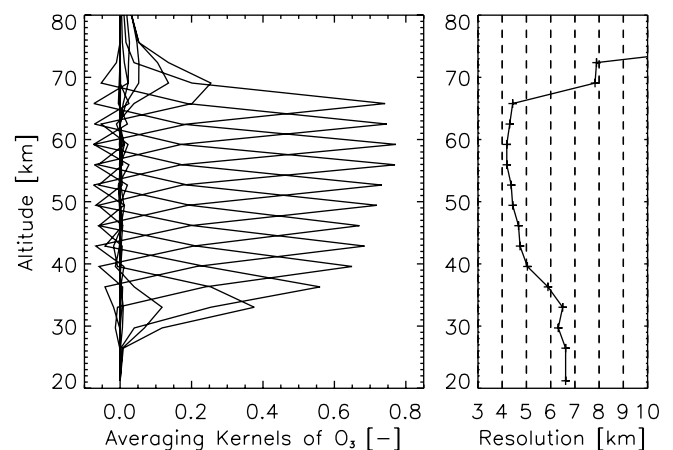


Fig. 3. Averaging kernels and calculated vertical resolution of a retrieved profile, as given by the Full Width at Half Maximum (FWHM) of the averaging kernels obtained from a sample ozone profile retrieval (same observation as in Figs. 1 and 2). The resolution between 40 and 65 km is less than 5 km.

Table 1
Overview of error sources (%)

Altitude	35 km	39 km	45 km	51 km	57 km	65 km
Single scattering ^a	3	1	0.3	0.1	0.1	0.05
A priori ^b	12	1	3	2.5	3	7
Ground albedo (A) ^c	2	0.6	0.1	0.02	0.01	0.01
Background density ^d	0.7	1.2	0.7	0.2	0.1	0.1
Temperature ^e	10	7	3	2	1	3
Pointing errors ^f	4	10	15	16	17.5	19
Solar zenith angle ^g	0.6	0.3	0.4	0.5	0.3	0.2
Solar zenith angle ^h	12	10	9	10	9	7
Cross-sections ⁱ	4	7	5	2	1	2

^a Neglecting multiple scattering and reflection.

^b Change of 100%.

^c Changing from $A = 0$ to $A = 0.5$.

^d 20% decrease.

^e $\Delta T = 40$ K.

^f $\Delta h = 0.5$ km.

^g Changing from 50° to 48° .

^h Changing from 84° to 82° .

ⁱ Temperature-dependent, $\Delta T = 40$ K.

185 ozone profiles up to 60 km. While the MIPAS ozone
186 concentrations are in general 2–15% higher than ozone
187 concentrations from HALOE, the SCIAMACHY ozone
188 concentrations in the altitude region from 38 to 55 km are
189 about 10% lower than MIPAS and 20% less below and above
190 this limits (see Figs. 4 and 5).

191 5. Ozone depletion during the Solar Proton Event (SPE) in 192 October/November 2003

193 Between 28 October 2003 and 4 November 2003 the
194 largest solar flares of the solar cycle 23 to date occurred
195 causing a big particle and radiation storm on Earth. Deple-
196 tion of ozone by an SPE was first observed by Weeks et al.
197 (1972). Swider and Kenesha (1973) suggested the produc-
198 tion of odd hydrogen as a cause of the observed ozone
199 depletion. Crutzen and Solomon (1980) and Solomon
200 and Crutzen (1981) gave the first reasonable model predic-

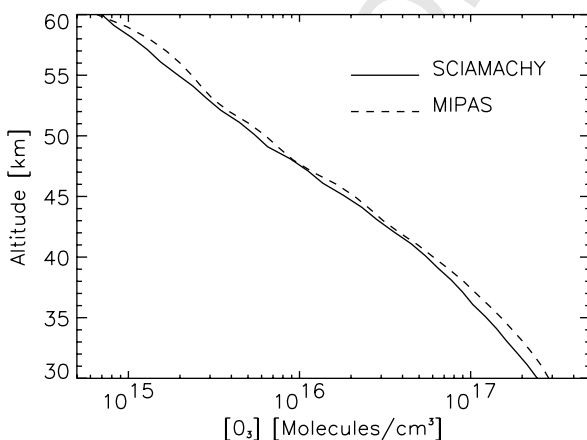


Fig. 4. Comparison of mean ozone profiles retrieved from all 434 local coincident SCIAMACHY V2.16 and MIPAS V4.61 measurements in March, 2004. The local coincidence of the particular MIPAS measurement is within 500 km radius around the SCIAMACHY tangent point and is further restricted to 2° difference in the solar zenith angles.

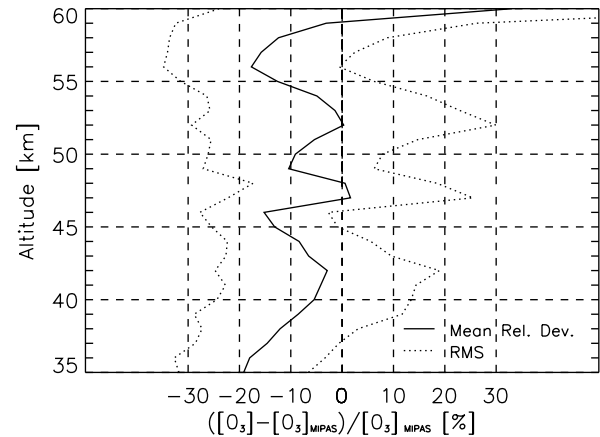


Fig. 5. Validation statistics of mean ozone profiles retrieved from SCIAMACHY limb spectra in comparison to the 434 collocated operational MIPAS V4.61 ozone profiles of March, 2004. The coincidence criteria are the same as in Fig. 4. Except for an altitude of 45 km the mean relative deviation is below 10% in altitudes from 37 to 55 km. The ranges above and below exceed deviations of 20%.

201 tions to explain the mechanism for the ozone depletion
202 observed with SME. Another detailed observation of the
203 SPE on 13 July, 1982 (Thomas et al., 1983) with SME
204 has been discussed by Solomon et al. (1983): highly ener-
205 getic protons ionize the air and produce HO_x and NO_x
206 constituents through complicated water cluster chemistry.
207 HO_x is responsible for the depletion during the first days,
208 while NO_x can have an effect over months or longer and
209 can be transported downward into the stratosphere (Crut-

SPE Induced Ozone Change [%] at 49 km
28 Oct - 5 Nov. 2003

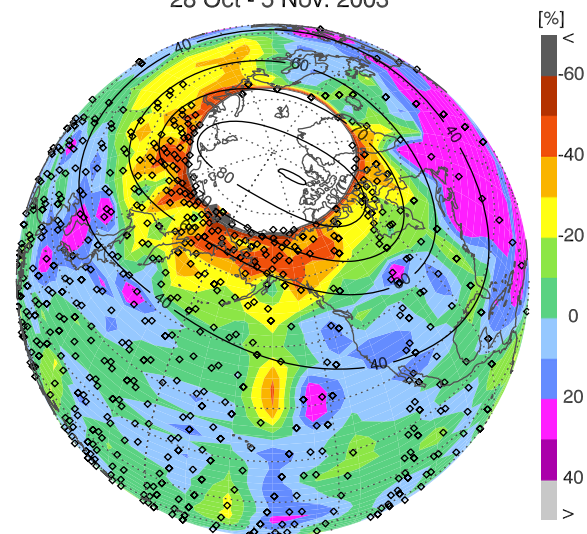


Fig. 6. Ratio of averaged ozone concentrations at an altitude of 49 km in the Northern hemisphere during the SPE (28 October to 6 November) and during a reference period (20–24 October) before the SPE. The Earth's magnetic latitude lines (black lines) were produced by the World Magnetic Model (WMM) (Macmillan and Quinn, 2000). The diamonds indicate the locations of SCIAMACHY limb scattering observations. The polar region in the Northern hemisphere is not covered by SCIAMACHY limb scatter observations due to an inclination angle of 98.55° , and because the Pole is not sunlit in early November.

SPE Induced Ozone Change [%] at 49 km
29 - 30 Oct. 2003

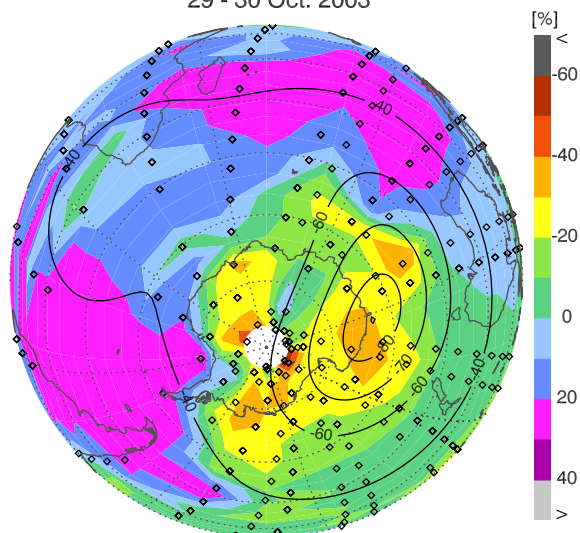


Fig. 7. In the Southern hemisphere, evident changes of the ozone concentrations can only be observed in a period from 29 to 30 October 2003. The ozone depletion is mainly located where the solar particles penetrate the atmosphere at the magnetic poles. Descriptions are the same as in Fig. 6.

zen et al., 1975). A newer review of the investigations can be found, e.g., in Jackman and McPeters (2004).

In limb viewing geometry SCIAMACHY observes at tangent points which are about 3000 km away from the sub-satellite point, so the impact of radiation hits on the analysed ozone profiles is reduced. In the dataset no indications of radiation hits which may affect the profile retrieval were found.

Figs. 6 and 7 show the depletion of ozone at 49 km in the Northern and Southern hemisphere. In the Southern hemisphere the ozone depletion can only be seen clearly during the first part of the event from 29 to 30 October. In contrast to the observations in the Southern hemisphere, the depletion in the north is stronger and can be seen over the whole particle precipitation period from 28 October to 7 November 2003. The hemispheric difference is in part due to a different ambient HO_x production, which is a consequence of the differences in the solar zenith angles. More ambient (not SPE produced) HO_x is present in the Southern hemisphere, leading to lower ambient ozone levels. Therefore the impact of the SPE produced HO_x will relatively not be as severe. A clear correlation of the ozone depletion and the strength of the Earth's magnetic field is observed (see Fig. 7 and explanations in the caption of Fig. 6).

6. Conclusions

The retrieval version V2.16 of upper stratospheric/lower mesospheric ozone profiles with thirteen selected wavelengths in the Hartley bands of ozone provides reliable profiles of ozone concentrations from 35 to 65 km. A first validation with ozone profiles retrieved from the MIPAS

instrument shows a good agreement. The main error sources of the retrieved ozone profiles have been estimated. Furthermore we described the ozone depletion caused by the SPE at the end of October and in the beginning of November 2003 with maxima of about 60% in the Northern hemisphere and of about 40% in the Southern hemisphere. In the Southern hemisphere a correlation of the ozone depletion and the Earth's magnetic field was observed.

Acknowledgements

Parts of this work have been funded by the German Ministry of Education and Research BMBF (Grant 07UFE12/8) and the German Aerospace Centre DLR (Grant 50EE0027). We would also like to thank ESA for providing the operational MIPAS ozone profiles for validation.

References

- Bovensmann, H., Burrows, J.P., Frerick, J., Noël, S., Rozanov, V.V., Chance, K.V., Goede, A.P.H. SCIAMACHY: mission objectives and measurements modes. *J. Atmos. Sci.* 56 (2), 127–148, 1999.
- Bracher, A., Bramstedt, K., Sinnhuber, M., Weber, M., Burrows, J.P. Validation of MIPAS O_3 , NO_2 , H_2O and CH_4 profiles (V4.61) with collocated measurements of HALOE and SAGE II, in: ESA Second Workshop on the Atmospheric Chemistry Validation of ENVISAT (ACVE-2), Frascati, Italy. SP-562. Noordwijk, Netherlands, p. 319, 2004.
- Crutzen, P.J., Isaksen, I.S.A., Reid, G.C. Solar proton events: stratospheric sources of nitric oxide. *Science* 189, 457–458, 1975.
- Crutzen, P.J., Solomon, S. Response of mesospheric ozone to particle precipitation. *Planet. Space Sci.* 28, 1147–1153, 1980.
- Eichmann, K.-U., Kaiser, J.W., von Savigny, C., Rozanov, A., Rozanov, V.V., Bovensmann, H., König, M., Burrows, J.P. v. SCIAMACHY limb measurements in the UV/V is spectral region: first results. *Adv. Space Res.* 34 (4), 744–748, 2004.
- Fischer, H., Oelhaf, H. Remote sensing of vertical profiles of atmospheric trace constituents with MIPAS limb-emission spectrometers. *Appl. Opt.* 35 (16), 2787–2796, 1996.
- Flittner, D.E., Bhartia, P.K., Herman, B.M. O_3 profiles retrieved from limb scatter measurements: theory. *Geophys. Res. Lett.* 27 (17), 2601–2604, 2000.
- Jackman, C.H., McPeters, R.D. The effect of solar proton events on ozone and other constituents, in: *Solar Variability and its Effects on Climate*. No. 10.1029/141GM21. American Geophysical Union, pp. 305–319, 2004.
- Janz, S.J., Hilsenrath, E., Flittner, D., Heath, D. Rayleigh scattering attitude sensor. *Proc. Spie* 2831, 146–153, 1996.
- Kaiser, J.W. Atmospheric parameter retrieval from UV–vis–NIR limb scattering measurements. Ph.D. thesis, University of Bremen, 2001.
- Kaiser, J.W., von Savigny, C., Eichmann, K.-U., Noël, S., Bovensmann, H., Burrows, J.P. Satellite-pointing retrieval from atmospheric limb-scattering of solar UV-B radiation. *Can. J. Phys.* 82, 1041–1052, 2004.
- Kaufmann, M.O., Gusev, O.A., Grossmann, K.U., Martin-Torres, F.J., Marsh, D.R., Kutepov, A.A. Satellite observations of daytime and nighttime ozone in the mesosphere and lower thermosphere. *J. Geophys. Res.* 108 (D9), 4272–4285, 2003.
- Kyrölä, E., Tamminen, J., Leppelmeier, G.W., Sofieva, V., Hassinen, S., Bertaux, J.L., Hauchecorne, A., Dalaudier, F., Cot, C., Korablev, O., d'Anton, O.F., Barrot, G., Mangin, A., Théodore, B., Guirlet, M., Etanchaud, F., Snoeij, P., Koopman, R., Saavedra, L., Fraisse, R., Fussen, D., Vanhellmont, F. GOMOS on Envisat: an overview. *Adv. Space Res.* 33 (7), 1020–1028, 2004.

- Li, D., Shine, K.P. A 4-dimensional ozone climatology of ozone for UGAMP models. UGAMP internal report 35, British Geological Survey, Department of Meteorology, University of Reading, 1995.
- Llewellyn, E.J., Lloyd, N.D., Degenstein, D.A., Gattinger, R.L., Petelina, S.V., Bourassa, A.E., Wiensz, J.T., Ivanov, E.V., McDade, I.C., Solheim, B.H., McConnell, J.C., Haley, C.S., von Savigny, C., Sioris, C.E., McLinden, C.A., Evans, W.F.J., Puckrin, E., Strong, K., Wehrle, V., Hum, R.H., Kendall, D.J.W., Matsushita, J., Murtagh, D.P., Brohede, S., Stegman, J., Witt, G., Barnes, G., Payne, W.F., Piché, L., Smith, K., Warshaw, G., Deslauniers, D.-L., Marchand, P., Richardson, E.H., King, R.A., Wever, I., McCreath, W., Kyrölä, E., Oikarinen, L., Leppelmeier, G.W., Auvinen, H., Mégie, G., Hauchcorne, A., Lefèvre, F., de La Nöe, J., Ricaud, P., Frisk, U., Sjöberg, F., von Schéele, F., Nordh, L. The OSIRIS instrument on the Odin spacecraft. *Can. J. Phys.* 82 (6), 411–422, 2004.
- Llewellyn, E.J., Witt, G. The measurements of ozone concentrations at high latitudes during the twilight. *Planet. Space Sci.* 25 (2), 165–172, 1977.
- López-Puertas, M. Definition of observational requirements for support to a future Earth explorer atmospheric chemistry mission. Tech. Rep. ESTEC Contract Number 13048/98/NL/DG, WP 6000: Molecular Non-Local Thermodynamic Equilibrium Working Document V2.0, Instituto de Astrofísica de Andalucía (CSIC), Granada, Spain, 2000.
- Macmillan, S., Quinn, J.M., The derivation of World Magnetic Model 2000. Tech. Rep. WM/00/17R, British Geological Survey, Edinburgh, 2000.
- Marsh, D.R., Skinner, W.R., Marshall, A.R., Hays, P.B., Ortland, D.A., Yee, J.-H. High Resolution Doppler Imager observations of ozone in the mesosphere and lower thermosphere. *J. Geophys. Res.* 107 (D19), 4390, 2002.
- McPeters, R. Ozone profile comparisons, in: The atmospheric effects of stratospheric aircraft: Report of the 1992 models and measurement workshop. No. 1292 in NASA Reference Publ. M.J. Prather, E.E. Remsberg, pp. D31–D37, 1993.
- McPeters, R.D., Janz, S.J., Hilsenrath, E., Brown, T.L., Flittner, D.E., Heath, D.F. The retrieval of O₃ profiles from limb scatter measurements: results from the Shuttle Ozone Limb Sounding Experiment. *Geophys. Res. Lett.* 27 (17), 2597–2600, 2000.
- Noxon, J.F. Twilight enhancements in O₂(b¹Σ_g⁻) emission. *J. Geophys. Res.* 80, 1370–1373, 1975.
- Rusch, D.W., Mount, G.H., Barth, C.A., Thomas, R.J., Callan, M.T. Solar Mesosphere Explorer Ultraviolet Spectrometer: Measurements of ozone in the 1.0-0.1 mbar region. *J. Geophys. Res.* 89 (D7), 11677–11687, 1984.
- Russell, J.M., Tuck, A.F., Gordley, L.L., Park, H.H., Drayson, S.R., Hesketh, D.H., Cicerone, R.J., Frederick, J.E., Harries, J.E., Crutzen, P.J. The Halogen Occultation Experiment. *J. Geophys. Res.* 98 (D6), 10777–10797, 1993.
- Solomon, S., Crutzen, P.C. Analysis of the August 1972 solar proton event including chlorine chemistry. *J. Geophys. Res.* 86, 1140–1146, 1981.
- Solomon, S., Reid, G.C., Rusch, D.W., Thomas, R.J. Mesospheric ozone depletion during the solar proton event of July 13, 1982. Part II. Comparison between theory and measurements. *Geophys. Res. Lett.* 10, 257–260, 1983.
- Swider, W., Kenesha, T.J. Decrease of ozone and atomic oxygen in the lower mesosphere during a PCA event. *Planet. Space Sci.* 21, 1969, 1973.
- Thomas, R.J., Barth, C.A., Rottman, G.J., Rusch, D.W., Mount, G.H., Lawrence, G.M. Ozone densities in the mesosphere (50-90 km) measured by the SME limb scanning near infrared spectrometer. *Geophys. Res. Lett.* 20, 245, 1983.
- von Savigny, C., Haley, C.S., Sioris, C.E., McDade, I.C., Llewellyn, E.J., Degenstein, D., Evans, W.F.J., Gattinger, R.L., Griffioen, E., Kyrölä, E., Lloyd, N.D., McConnell, J.C., McLinden, C.A., Mégie, G., Murtagh, D.P., Solheim, B., Strong, K. Stratospheric ozone profiles retrieved from limb scattered sunlight radiance spectra measured by the OSIRIS instrument on the Odin satellite. *Geophys. Res. Lett.* 30 (14), 1755, 2003.
- von Savigny, C., Kaiser, J.W., Bovensmann, H., Burrows, J.P., McDermond, I.S., Leblanc, T. Spatial and temporal characterization of SCIAMACHY limb pointing errors during the first three years of the mission. *Atmos. Chem. Phys.* 5, 2593–2602, 2005.
- von Savigny, C., Kokhanovsky, A., Bovensmann, H., Eichmann, K.-U., Kaiser, J., Noël, S., Rozanov, A.V., Skupin, J., Burrows, J.P. NLC detection and particle size determination: first results from SCIAMACHY on Envisat. *Adv. Space Res.* 34, 851–856, 2004a.
- von Savigny, C., Rozanov, A., Bovensmann, H., Eichmann, K.-U., Noël, S., Rozanov, V.V., Sinnhuber, B.-M., Weber, M., Burrows, J.P. The ozone hole break-up in September 2002 as seen by SCIAMACHY on ENVISAT. *J. Atmos. Sci.* 62 (3), 721–734, 2004b.
- Weeks, L.H., Chuikay, R.S., Corbin, J.R. Ozone measurements in the mesosphere during the solar proton event of 2 November 1969. *J. Atmos. Sci.* 29, 1138–1142, 1972.